Asian Journal of Chemistry; Vol. 26, No. 10 (2014), 2839-2844

ASIAN JOURNAL OF CHEMISTRY

http://dx.doi.org/10.14233/ajchem.2014.15813

Removal of Water from Anisole by 3A Molecular Sieve in Batch and Fixed-bed Column Systems

NA SUN*, PENG BAI, XIANGHAI GUO and LEI WANG

School of Chemical Engineering and Technology, Tianjin University, Tianjin 300072, P.R. China

*Corresponding author: Tel: +86 15922295983; E-mail: sunflowersls@hotmail.com

Received: 22 May 2013; *Accepted*: 22 July 2013; *Published online*: 10 May 2014; AJC-15130

3A molecular sieve, conducted by three thermodynamic and two kinetic adsorption experiments for testing its adsorption ability, was the adsorbent for the removal of trace of H_2O from anisole solution in both batch and fixed-bed column operations. The effects of flow rate, initial H_2O concentration and bed height on the adsorption characteristics of 3A molecular sieve in the fixed-bed column system were investigated. Data analysis confirmed that the breakthrough curves were dependent on the three factors. Three kinetic models, namely Thomas, Yoon-Nelson and Adams-Bohart, were applied to experimental data to predict breakthrough curves and to determine the column characteristic parameters that were useful for process design. The data were in good agreement with the Thomas and Yoon-Nelson models. It was concluded that 3A molecular sieve could be used to remove trace H_2O in anisole solution.

Keywords: Anisole, Adsorption, 3A molecular sieve, Fixed-bed column.

INTRODUCTION

Anisole is a widely used organic chemical material and often used as an organic reagent, solvent, spice and repellent. The main product of anisole allylation is used in perfumes and the flavoring agent in food and liquors[1]. Mesoporous Al MCM-41 molecular sieve is synthesized with anisole catalyst[2]. Industrial production of enriching isotope ^{10}B is based on the separation of trifluoride-anisole complex by chemical exchange distillation. The H_2O content in anisole complex agent is required to be very small. The H_2O content of anisole solution generally ranges from 0.04 to 0.05 % (weight per cent), it should be dehydrated to a H_2O content of 0.002 to 0.003 %[3]. Trace water interferes with the reuse of anisole and affects the quality of downstream products. Further dehydration of anisole becomes a problem to be solved. When mass fraction of H_2O at 0.4-99 % in anisole, the water-anisole mixture is a heteroazeotrope, the composition of the vapor phase is constant and is equal to 40.5 mass % of H_2O[3], therefore a general rectification method cannot be used to get high purity anisole[4]. Air stripping method is used generally in industrial production process for the removal of trace components in mixture. The process of removing trace of H_2O in anisole solution by nitrogen gas stripping method is relatively complex, consuming a large quantity of nitrogen and not economical[4]. Adsorption is an important chemical separation unit operation which has more competitive advantages in simple operation, low energy consumption, a high degree of purification and flexibility of automatic control than the conventional separation processes. Compared with other adsorbents, 3A molecular sieve has the advantages of high selectivity and adsorption capacity[5]. Its crystal structure has orderly and uniform pores whose size are the magnitude of molecular size, which only allows the molecules having smaller size to go into, so a mixture of molecules can be screened by size. In low-pressure, low-concentration, high-temperature or other harsh conditions, especially for H_2O, it still has high adsorption capacity. The aim of the present work is to explore the possibility of utilizing 3A molecular sieve for the removal of H_2O from anisole solution. The thermodynamic and kinetic models have been applied to the adsorption data. The effects of flow rate, initial H_2O concentration and bed height on H_2O adsorption by 3A molecular sieve column were investigated. Thomas, Adams-Bohart and Yoon-Nelson models were also used to predict the adsorption performance of the fixed-bed column system.

EXPERIMENTAL

Preparation of adsorbent: The beaker was charged with an amount of 3A molecular sieves which were prepared to be activated in a vacuum oven at 150 ºC under the vacuum degree of 0.1 Mpa for 5 h. After fully activated, they were cooled to around 20 ºC in a desiccator with the protection of the dry nitrogen, whose flow rate was 150 cm^3/min in the cooling process.

Batch thermodynamic studies: The batch experiments were to detect the relationship of equilibrium concentration

and equilibrium adsorption capacity to obtain adsorption isotherm. The experiments were carried out by adding 2 g of 3A molecular sieves into a series of 500 mL flasks filled with 200 mL anisole solution of which H_2O contents were 600, 700, 800, 900 and 1000 mg/L, respectively, under stirring condition of 100 rpm at 298 and 308 K till equilibrium. The remaining concentration of the H_2O was analyzed by Moisture Analyzer until equilibrium had been reached for half one day. The amount of adsorption of H_2O at equilibrium q_e (mg/g) was calculated by using the following eqn. 1 in batch sorption system:

$$q_e = \frac{(C_o - C_e)V}{M} \quad (1)$$

where q_e (mg/g) is the amount of H_2O adsorbed in molecular sieve per g at equilibrium. C_o and C_e (mg/L) are the liquid-phase concentrations of H_2O at initial and equilibrium conditions, respectively. V (L) is the volume of the solution and W (g) is the mass of 3A molecular sieve.

Batch kinetic studies: Adsorption kinetics experiments, which were conducted to study the relationship between time and adsorption capacity, were carried out in the special 250 mL flasks, equal amounts of 3A molecular sieves (4g) were loaded in 200 mL anisole solution with H_2O contents were 450, 610, 730 and 900 mg/L at 298 K. In order to eliminate the influence of external diffusion, kept the stirring speed at 300 rpm. At predetermined intervals of time, solutions were analyzed for the final concentration of H_2O, it was defined as the adsorption end point that H_2O concentration no longer changed within 0.5 h. The amount of adsorption q_t (mg/g), at time t (h), was calculated by:

$$q_t = \frac{(C_o - C_t)V}{W} \quad (2)$$

where C_t (mg/L) is concentrations of H_2O at time t.

Fixed-bed adsorption studies: Fig. 1 represented the schematic diagram of the fixed-bed adsorption system. Continuous flow adsorption studies were conducted in a column made of Pyrex glass tube with inner diameter of 2cm and fixed bed height (50, 75 and 100 cm). A sieve made up of stainless steel was placed at the bottom of the column. Above the stainless steel sieve, a layer of glass wool was placed to prevent loss of adsorbent. A peristaltic pump was used to pump the feed (H_2O content was 550, 900 and 1200 ppm, respectively) upward through the column at a desired flow rate (4, 8 and 12 mL/min). The solution was pumped upward to avoid channeling due to gravity.

RESULTS AND DISCUSSION

Batch thermodynamic studies: Batch thermodynamic data of 3A were obtained at 298 K, 308 K and were analyzed by the linear form of Langmuir isotherm equation[6,7] which is expressed by:

$$\frac{C_e}{q_e} = \frac{1}{q_{max} K_L} + \frac{C_e}{q_{max}} \quad (3)$$

where q_{max} (mg/g) is the maximum amount of the H_2O per unit weight of 3A molecular sieve to form a complete monolayer on the surface. Whereas K_L (L/mg) is Langmuir constant related to the affinity of the binding sites.

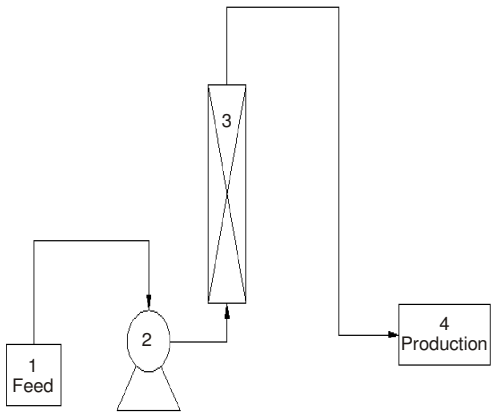

1 Anisole tank 2 Constant flow pump 3 Adsorption column 4 Production tank

Fig. 1. Fixed-bed adsorption system

The essential characteristics of the Langmuir isotherm can be expressed in terms of a dimensionless constant separation factor R_L[8] which is given by

$$R_L = \frac{1}{1 + C_o K_L} \quad (4)$$

where C_o is the highest initial concentration of adsorbate (mg/L) and K_L (L/mg) is Langmuir constant. The value of R_L indicates the shape of the isotherm to be either unfavorable ($R_L > 1$), linear ($R_L = 1$), favorable ($0 < R_L < 1$), or irreversible ($R_L = 0$). The R_L values between 0 and 1 indicate favorable adsorption[9].

The equation of Freundlich isotherm[10,11] is an empirical model employed to describe heterogeneous systems. This gives an expression encompassing the surface heterogeneity and the exponential distribution of active sites and their energies. The Freundich equation is

$$q_e = K_F C_e^{1/n} \quad (5)$$

where K_F (mg/g (L/mg)) and 1/n are Freundlich constants with sorbent adsorption capacity and the constant indicative of the intensity of the adsorption process. Values of $1/n < 1$ represent favorable adsorption condition[12,13]. They can be determined from the linear plot of ln q_e *versus* ln C_e.

Temkin isotherm[9] assumes that the adsorption heat linearly decreases as the adsorption quantity increases and the adsorption binding energy is distributed uniformly[14,15]. It has been used in form of eqns. 6 and 7 presents its linearized form:

$$q_e = \frac{RT}{b} \ln(AC_e) \quad (6)$$

$$q_e = \frac{RT}{b} \ln A + \frac{RT}{b} \ln C_e \quad (7)$$

Here RT/b = B, which is Temkin constant related to heat of sorption, whereas A (L/g) represents the equilibrium binding constant corresponding to the maximum binding energy. R (8.314 J/(mol K)) is universal gas constant and T (K) is absolute temperature. The values of the Temkin constants A and B were calculated by plotting q_e *versus* ln C_e from eqn. 7. The model parameters of three types of molecular sieves at different temperature are listed in Table-1.

TABLE-1
MODEL PARAMETERS OF 3A MOLECULAR SIEVE AT 298 AND 308 K

Isotherm model	Parameters	Temperature (K)	
		298	308
Langmuir	q_{max}	93.05	89.25
	K_L	0.0288	0.0162
	R_L	0.0506	0.0714
	R^2	0.9971	0.9964
Freundlich	K_F	15.28	8. 6313
	1/n	0.3306	0.4128
	R^2	0.9774	0.9900
Temkin	A(L/g)	0.1943	0.0145
	B	23.46	24.96
	R^2	0.9862	0.9917

Table-2 suggested that K_L decreases with the rise of temperature. The R_L value obtained is less than 1, which demonstrates that the adsorption of H_2O on 3A molecular sieve is favorable. Freundlich exponent, 1/n, ranging between 0 and 1, shows favorable adsorption of H_2O onto the surface of 3A molecular sieves. Moreover, 3A molecular sieve has a large Temkin constant B, hence 3A molecular sieve is suitable for the adsorption of H_2O from anisole. Fig. 2 shows the plots comparing the Langmuir, the Freundich and the Temkin isotherm with experimental data at 298 and 308 K.

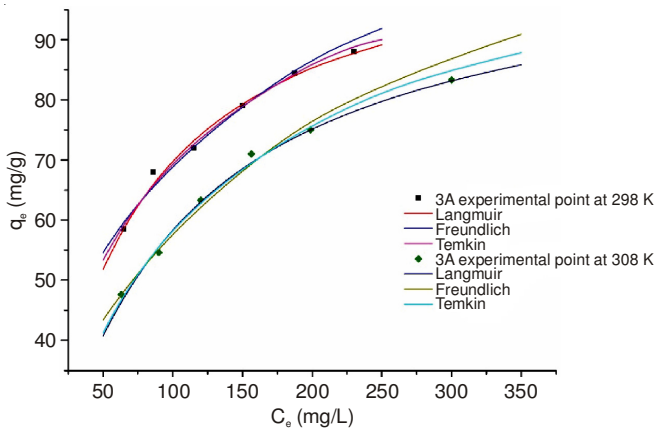

Fig. 2. Theoretical curves of Langmuir, Freundlich and Temkin isotherms with the experimental points at 298 and 308 K

From Fig. 2 and R^2 of Table-1, Langmuir isotherm shows an excellent fit with the experimental data than Freundlich and Temkin isotherms and q_e at 285 K is larger than that at 308 K under the different equilibrium concentrations C_e, indicating that q_e complies with the law that high temperature is not conducive to adsorption.

Batch kinetics studies: The model of adsorption kinetics of H_2O on molecular sieve was investigated by two common models, namely, the Lagergren pseudo-first-order model[11,16] and pseudo-second-order model[17,18]. Lagergren proposed a method for adsorption analysis which is the pseudo-first-order kinetic equation in the linear form:

$$\log(q_e - q_t) = \log q_e - \left(\frac{k_1}{2.303}\right)t \quad (8)$$

where q_e and q_t are the amounts of H_2O adsorbed at equilibrium in mg/g and time in h, respectively and k_1 is the pseudo-first-order rate constant (1/h). A linear plot of log (q_e - q_t) against time t allows one to obtain the rate constant. The Lagergren's pseudo-first-order rate constant k_1 and q_e were displayed in Table-2.

The pseudo-second-order kinetics can be expressed as[17,18]:

$$\frac{t}{q_t} = \frac{1}{k_2 q_e^2} + \left(\frac{1}{q_e}\right)t \quad (9)$$

where k_2 (g/mg h) is the rate constant of adsorption, q_e (mg/g) is the amount of H_2O adsorbed at equilibrium and q_t (mg/g) is the amount of H_2O adsorbed at time t. The equilibrium adsorption capacity q_e and the second-order constants k_2 (g/mg h) can be determined experimentally from the slope and intercept of plot t/q_t *versus* t. The k_2 and q_e determined from the model are presented in Table-2 along with corresponding correlation coefficients.

With the increasing of initial concentration, q_e increases gradually, k_1 and k_2 have the tendency to decrease. Fig. 3 shows the relationship of theoretical curves of the pseudo-first-order model and pseudo-second-order model with the experimental points at different initial concentration.

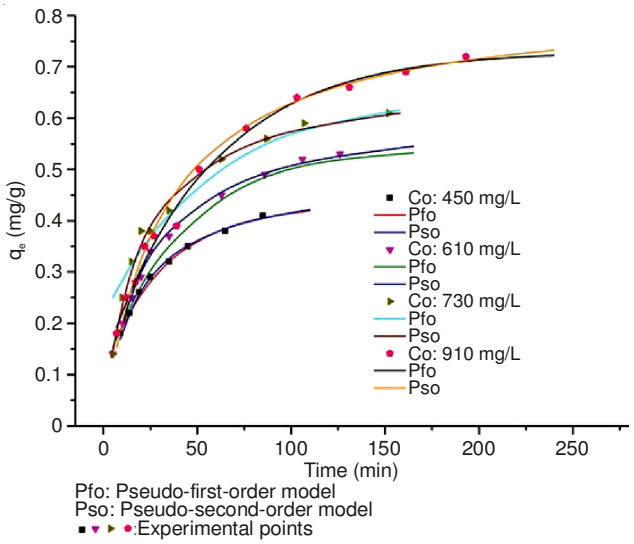

Fig. 3. Effect of contact time on adsorption of H_2O at different initial concentration

TABLE-2
COMPARISON OF q_e VALUES UNDER THE PSEUDO-FIRST-ORDER MODEL AND PSEUDO-SECOND-ORDER MODEL

Initial concentration (mg/L)	$q_{e,exp}$ (mg/g)	Pseudo-first-order kinetic model			Pseudo-second-order kinetic model		
		k_1 (1/h)	$q_{e,cal}$ (mg/g)	R^2	k_2 (g/mg h)	$q_{e,cal}$ (mg/g)	R^2
450	0.43	1.8767	0.3244	0.9902	7.5251	0.4825	0.9986
610	0.54	1.4771	0.4380	0.997	4.6633	0.6144	0.997
730	0.64	1.0944	0.4276	0.9789	4.7592	0.6814	0.9988
910	0.74	1.0412	0.6102	0.9889	2.3530	0.8268	0.9988

Observed from Fig. 3 and correlation coefficients in Table-2, suggested that the pseudo-second-order model better represented the adsorption kinetics and the calculated q_e values agreed more with the experimental q_e values. This suggested that the adsorption of H_2O follows second-order kinetics model.

Fixed bed adsorption study: Breakthrough curves for adsorption of H_2O from anisole solution on 3A molecular sieve for different conditions are represented in Fig. 4 and related parameters of breakthrough curves for different conditions are listed in Table-3.

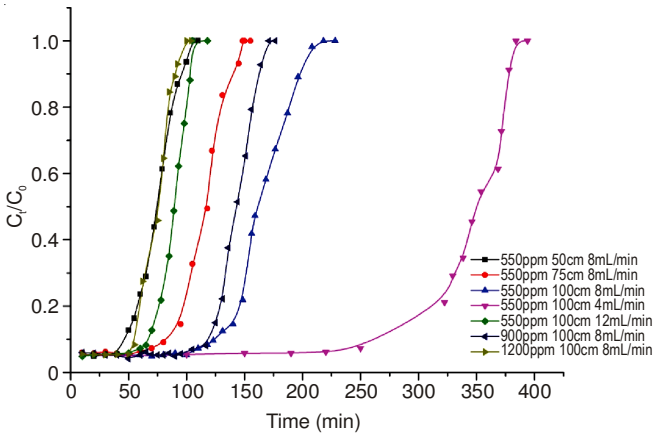

Fig. 4. Breakthrough curves for adsorption of H_2O from anisole solution on 3A molecular sieve for different conditions

The experimental results show that the concentrations before the breakthrough can meet the requirements of 0.002 % to 0.003 % (weight per cent) under different conditions.

The effect of feed flow rate on the adsorption of H_2O in the anisole solution on 3A molecular sieve was investigated by changing the feed flow rate (4, 8 and 12 mL/min) with constant adsorbent bed height of 100 cm and inlet adsorbate concentration of 550 mg/L, as shown by the breakthrough curve in Fig. 4 and parameters in Table-3 where it can been seen that q_e, the breakthrough and exhaustion times decrease with a higher flow rate. The slope of the breakthrough curves increase as the flow rate increases. The reason is that total adsorption capacity of the bed is constant, therefore, the lower flow speed, the longer retention time, H_2O has more chances to be in contact with adsorbent, which is resulted in a greater removal of H_2O molecules in column and the increase of the amount of the adsorbate in the unit time in the bed.

The effect of adsorbate H_2O concentration on the column performance was studied by testing the inlet concentration of 550, 900 and 1200 mg/L for the same adsorbent bed height of 100 cm and feed flow rate of 8 mL/min. The breakthrough and exhaustion time decrease as the influent H_2O concentration increases, but q_e has the opposite trend. As the inlet H_2O concentration increases, much sharper breakthrough curve is observed. The lower H_2O concentration results in a delayed breakthrough curve since the lower concentration gradient causes reduced transport of H_2O. The driving force for adsorption is the concentration gradient between the solute on the adsorbent and the solute in the solution[19,20]. High concentration gradient provides a higher driving force, which favours the adsorption process. Therefore, when H_2O uptake is desired, which is often the case, operating with high initial H_2O concentrations appears to be favorable.

The breakthrough curve obtained for adsorption of H_2O on 3A molecular sieve for different bed height of 50, 75 and 100 cm at constant adsorbate feed flow rate of 8 mL/min and inlet concentration 550 mg/L. Fig. 4 shows that both the breakthrough and exhaustion times increase as the bed height increases, q_e has the same tendency. The slope of the breakthrough curve decreases as the bed height increases. This can be traced to an increase in the axial dispersion of the anisole over the column with an increase in column height[21]. The increases in bed height results in an increase in the volume of the anisole solution treated due to the increase in the specific surface of 3A molecular sieve which provides more fixation binding sites for the H_2O to be absorbed. The increase in the adsorbent mass in a higher bed provides a greater service area and thus leads to a higher percentage of H_2O removal and adsorption capacity q_e. So, a higher bed height can be chosen at a constant flow rate and inlet concentration.

Column dynamic studies: Three kinetic models, Thomas, Adams-Bohart and Yoon-Nelson, were applied to predict the breakthrough curves by using linear regression and to determine the characteristic parameters of the column that are useful for process design[22].

Application of Thomas model: The maximum adsorption capacity of an adsorbent is needed in design. Traditionally, the Thomas model is preferred to achieve the purpose. The model is based on the assumption that the process follows Langmuir kinetics of adsorption-desorption with no axial dispersion[23].The main advantages of this model are its simplicity and reasonable accuracy in predicting the breakthrough curves under various operating conditions[24]. The data obtained from a column in continuous mode studies are used to calculate the equilibrium adsorption capacity of H_2O on adsorbent and the adsorption rate constant using the kinetic model developed by Thomas[22,25]. The expression by Thomas model for an adsorption column is given below:

TABLE-3
PARAMETERS OF BREAKTHROUGH CURVES UNDER DIFFERENT CONDITIONS

Initial concentration (mg/L)	Bed height (cm)	Flow rate (mL/min)	C_t (µg/g)	T_b (h)	T_e (h)	$q_{e,exp}$ (mg/g)
550	50	8	31	40.1	100.5	108.02
550	75	8	28	70.8	145.7	132.21
550	100	8	26	110.3	210.8	186.91
550	100	4	31	250.4	384.6	191.93
550	100	12	29	60.7	96.5	152.10
900	100	8	30	80.5	151.5	162.98
1200	100	8	29	50.9	99.0	188.28

T_b: Breakthrough time, T_e: Exhaustion time; $q_{e,exp}$: Adsorption capacity. C_t: Average concentration before breakthrough point.

$$\ln\left[\left(\frac{C_o}{C_t}\right)-1\right]=\left(\frac{k_{Th}q_e m}{Q}\right)-\left(\frac{k_{Th}C_o V_{eff}}{Q}\right) \quad (10)$$

where k_{Th} (mL/mg min) is the Thomas rate constant. q_e (mg/g) is the equilibrium adsorption capacity and m is the amount of adsorbent in the column. The k_{Th} and q_e values were calculated from slope and intercepts of linear plots of against using values from the column experiment (Figures not shown). The model parameters are listed in Table-4.

Table-4 showed the values of q become bigger but decreases with initial H_2O concentration increases. The reason is that the driving force for adsorption is the concentration gradient between the H_2O on the adsorbent and the H_2O in the solution[26,27]. The values of k_{Th} becomes bigger whereas the value of q_e decreases as the flow rate increases. With the bed depth increasing, the values of k_{Th} becomes smaller while the value of q_e increases. A similar trend had also been observed for sorption of methylene blue by phoenix tree leaf powder fixed bed column[22]. So lower flow rate, higher initial concentration, higher bed height would increase the adsorption of H_2O on the 3A column. Experimental $q_{e,exp}$ and Thomas model-predicted equilibrium uptake capacities q_e were in accordance. The well-fitting of the experimental data with the Thomas model indicates that the external and internal diffusion are not the limiting step[28].

Application of the Yoon-Nelson model: A simple theoretical model developed by Yoon-Nelson was applied to investigate the breakthrough behavior of H_2O on 3A molecular sieve. The model is based on the assumption that the rate of decrease in the probability of adsorption for each adsorbate molecule is proportional to the probability of the adsorbate adsorption and the adsorbate breakthrough on the adsorbent[28,29]. The Yoon–Nelson which is a linearized model for a single component system is expressed as:

$$\ln\frac{C_t}{C_o-C_t}=k_{YN}t-\tau k_{YN} \quad (11)$$

where k_{YN} (1/min) is the rate velocity constant, τ (min) is the time required for 50 % adsorbate breakthrough. A linear plot of ln $[C_t/(C_o - C_t)]$ against sampling time (t) determines values of k_{YN} and τ from the intercept and slope of the plot (figure not shown). The values of k_{YN} and τ are listed in Table-5.

From Table-5, the rate constants k_{YN} increase but the 50 % breakthrough times τ decrease as both the flow rate and H_2O inlet concentration increase. As the bed height increases, the values of τ increase while the values of k_{YN} decrease. The data in Table-5 also indicate that τ values from the calculation are almost the same compared to experimental results. High values of correlation coefficients indicate that Yoon and Nelson model fitted well to the experimental data. This is in agreement with the results obtained by Nwabanne and Igbokwe[30].

Application of the Adams-Bohart model: Adams-Bohart model[26] was established based on the surface reaction theory and it assumed that equilibrium was not instantaneous. Therefore the rate of adsorption was proportional to both the residual capacity of the 3A molecular sieve and the concentration of the absorbing species[31]. This model establishes the fundamental equations describing the relationship between C_t/C_o and t in a continuous system. The Adam's-Bohart model is used for the description of the initial part of the breakthrough curve. The mathematical equation of the model can be written as:

$$\ln\frac{C_t}{C_o}=k_{AB}C_o t-k_{AB}N_o\frac{Z}{F} \quad (12)$$

where C_o and C_t (mg/L) are the inlet and effluent H_2O concentration. k_{AB} (L/mg min) is the kinetic constant, F (cm/min) is the linear velocity calculated by dividing the flow rate by the column section area, Z (cm) is the bed height of column and N_o (mg/L) is the saturation concentration. A linear plot of ln C_t/C_o against time t was determined values of k_{AB} and N_o from the intercept and slope of the plot (figure not shown). For all breakthrough curves, respective values of N_o and k_{AB} were calculated and presented in Table-6 together with the correlation coefficients.

From Table-6, although the Adam's-Bohart model provides a simple and comprehensive approach to running and evaluating adsorption column test, its low correlation coefficient is

TABLE-4
THOMAS MODEL PARAMETERS FOR THE ADSORPTION OF H_2O AT DIFFERENT CONDITIONS

Initial conc. (mg/L)	Bed height (cm)	Flow rate (mL/min)	k_{Th} ($\times 10^{-3}$) (mL/mg min)	q_e (mg/g)	$q_{e,exp}$ (mg/g)	R^2
550	50	8	3.27	107.89	108.02	0.9883
550	75	8	2.73	131.92	132.21	0.9972
550	100	8	2.00	187.91	186.91	0.9965
550	100	4	1.09	191.92	191.93	0.9955
550	100	12	4.01	151.97	152.10	0.9895
900	100	8	2.11	163.95	162.98	0.9872
1200	100	8	1.67	189.28	188.28	0.9906

TABLE-5
YOON-NELSON PARAMETERS AT DIFFERENT CONDITIONS

Inlet concentration (mg/L)	Bed height (cm)	Flow rate (mL/min)	k_{YN} (1/min)	τ_{exp} (h)	τ_{cal} (h)	R^2
550	50	8	0.0018	74.60	74.18	0.9883
550	75	8	0.0015	116.05	115.04	0.9972
550	100	8	0.0011	160.15	162.26	0.9965
550	100	4	0.0006	340.10	341.05	0.9955
550	100	12	0.0022	89.50	88.27	0.9895
900	100	8	0.0019	142.50	142.65	0.9872
1200	100	8	0.0020	75.77	75.73	0.9906

TABLE-6
ADAM'S-BOHART PARAMETERS
AT DIFFERENT CONDITIONS

Inlet conc. (mg/L)	Bed height (cm)	Flow rate (mL/min)	k_{AB} ($\times 10^{-6}$) (L/mg min)	No ($\times 10^5$) (mg/L)	R^2
550	50	8	1.64	1.47	0.9010
550	75	8	1.45	1.51	0.9552
550	100	8	1.09	1.55	0.8747
550	100	4	0.54	1.86	0.9056
550	100	12	1.64	1.27	0.9702
900	100	8	1.20	1.61	0.8932
1200	100	8	1.00	1.83	0.9570

limited to the range of conditions. From Table-6, the values of k_{AB} increase with higher flow rate, lower bed height and inlet concentration, whereas larger flow rate, lower bed height and inlet concentration can lead to a smaller N_0.

Conclusion

3A molecular sieve is highly effective for removing H_2O in anisole solution in a fixed-bed system. Batch thermodynamic data followed Langmuir isotherm are better than that by Freundlich and Temkin isotherm at all temperature range being studied. Batch kinetics data is more suitable for pseudo-second-order kinetic model. A larger saturated adsorption capacity of 3A molecular sieve, a longer breakthrough and exhaustion time occur at a higher bed height, a lower influent H_2O concentration and flow rate. Column data are best-fitted with Thomas and Yoon-Nelson models than Adam's-Bohart model, so Thomas and Yoon-Nelson models can be used to determine the characteristic parameters of the column that are useful for process design.

REFERENCES

1. The Merck Index, edn. 13, p. 3740.
2. P. Kamala and A. Pandurangan, *Catal. Commun*., **9**, 2231 (2008).
3. V.A. Ivanov and S.G. Katalnikov, *Sep. Sci. Technol*., **36**, 1737 (2001).
4. J.-J. Liu, J. Xu, H.-L. Jia and W.-J. Zhang, *School Chem. Eng. Technol*., **39**, 42 (2011).
5. L.-D. Wang and Z.-R. Yin, *Liquor-making Sci. Technol.*, **109**, 24 (2002).
6. I. Langmuir, *J. Am. Chem. Soc*., **40**, 1361 (1918).
7. F. Xian-Cai and C. Qui-Hui, Physical Chemistry, Higher Press, China, pp. 303-321 (1988).
8. K.R. Hall, L.C. Eagleton, A. Acrivos and T. Vermeulen, *I&EC Fundam*, **5**, 212 (1966).
9. B.H. Hameed, J.M. Salman and A.L. Ahmad, *J. Hazard. Mater*., **163**, 121 (2009).
10. H.M.F. Freundlich, *Z. Phys. Chem.*, **57A**, 385 (1906).
11. I.A.W. Tan, A.L. Ahmad and B.H. Hameed, *Desalination*, **225**, 13 (2008).
12. R.E. Treybal, Mass Transfer Operations, McGraw Hill, New York, edn. 2 (1968).
13. Y.S. Ho and G. McKay, *Chem. Eng. J*., **70**, 115 (1998).
14. X.-S. Wang and Y. Qin, *Process Biochem*., **40**, 677 (2005).
15. R.D. Johnson and F.H. Arnold, *Biochim. Biophys. Acta*, **1247**, 293 (1995).
16. M. Hosseini, S.F.L. Mertens, M. Ghorbani and M.R. Arshadi, *Mater. Chem. Phys.*, **78**, 800 (2003).
17. Y.S. Ho, *J. Hazard. Mater*., **136**, 681 (2006).
18. Y.S. Ho and G. McKay, *Water Res*., **34**, 735 (2000).
19. J. Song, W. Zou, Y. Bian, F. Su and R. Han, *Desalination*, **265**, 119 (2011).
20. S.V. Gokhale, K.K. Jyoti and S.S. Lele, *J. Hazard. Mater.*, **170**, 735 (2009).
21. V.C. Taty-Costodes, H. Fauduet, C. Porte and Y.S. Ho, *J. Hazard. Mater.*, **123**, 135 (2005).
22. R. Han, Y. Wang, X. Zhao, Y. Wang, F. Xie, J. Cheng and M. Tang, *Desalination*, **245**, 284 (2009).
23. J. Song, W. Zou, Y. Bian, F. Su and R. Han, *Desalination*, **265**, 119 (2011).
24. T.E. Köse and N. Öztürk, *J. Hazard. Mater*., **152**, 744 (2008).
25. H.C. Thomas, *J. Am. Chem. Soc*., **66**, 1664 (1944).
26. A.A. Ahmad and B.H. Hameed, *J. Hazard. Mater*., **175**, 298 (2010).
27. T.V.N. Padmesh, K. Vijayaraghavan, G. Sekaran and M. Velan, *J. Hazard. Mater.*, **125**, 121 (2005).
28. Z.Z. Chowdhury, S.M. Zain, A.K. Rashid, R.F. Rafique and K. Khalid, *J. Chem.*, **Article ID 959761** (2013).
29. Y.H. Yoon and J.H. Nelson, *Am. Ind. Hygiene Assoc. J*., **161**, 1427 (2009).
30. J.T. Nwabanne and P.K. Igbokwe, *Int. J. Environ. Res*., **6**, 945 (2012).
31. G.S. Bohart and E.Q. Adams, *J. Chem. Soc*., **42**, 523 (1920).